

Sensor and Simulation Notes

Note 355  
(with corrections)

July 10, 1994

✓  
CLEARED  
FOR PUBLIC RELEASE  
PL/PA 15 JAN 97

The Balantenna: An Integrated Impedance  
Matching Network and Hybrid EMP Simulator

Donald P. McLemore  
Kaman Sciences Corporation

Gary D. Sower  
EG&G Special Projects

Carl E. Baum William D. Prather  
Phillips Laboratory

Abstract

This paper describes the integration of a matching circuit (balun) with the "wormhole" antenna feed concept for a hybrid CW EMP simulator described in previous work [1]. The amplifier for this system is still on the ground; however, at the gap of the antenna is a matching network which is designed to give the traditional 1:4 impedance ratio as found in previous designs [2,3,4]. With this design, matching for the antenna can be achieved up to the GHz regime.

PL 96 - 1160

Sensor and Simulation Notes

Note 355

January 20, 1993

The Balantenna: An Integrated Impedance  
Matching Network and Hybrid EMP Simulator

Donald P. McLemore  
Kaman Sciences Corporation

Gary D. Sower  
EG&G Special Projects

Carl E. Baum William D. Prather  
Phillips Laboratory

Abstract

This paper describes the integration of a matching circuit (balun) with the "wormhole" antenna feed concept for a hybrid CW EMP simulator described in previous work [1]. The amplifier for this system is still on the ground; however, at the gap of the antenna is a matching network which is designed to give the traditional 1:4 impedance ratio as found in previous designs [2,3,4]. With this design, matching for the antenna can be achieved up to the GHz regime.

CLEARED  
FOR PUBLIC RELEASE

PL/PA 9 Feb 93

PL 93-0077

## I. Introduction

Recent efforts to design and build hybrid EMP CW simulators have concentrated on simplicity and the ability to radiate high frequency energy with sufficient magnitude so that transfer functions for systems can be reliably measured at these higher frequencies. An antenna design which accomplishes these two objectives has been described in a previous note [1]. In this design, the "wormhole" feed concept was introduced, which allowed amplifiers for the simulator to be placed on the ground surface and the signal to the antenna is passed to a gap at the top of the antenna using the inner conductors of a high quality coaxial cable and the current on the external portion of the coaxial cable is controlled to the desired value using resistively loaded ferrite torroids. The currents which pass from the gap source to the outside surface of the shield of the coaxial cable become those responsible for creating the fields of the simulator (see fig. 1.1).

The next technical problem to be solved for this simulator is to design an impedance matching device to transition between the 50 ohm drive and the antenna impedance. Standard solutions for this problem have included quarter wave transmission line sections for narrowband applications [5], transformers (usually at lower frequencies) and short segments of transmission lines [3]. None of these traditional approaches, however, looked promising, since the matching network would have to be both broad band and fit into the small gap area of the antenna without disturbing the surrounding electromagnetic topology.

The most attractive alternative was to integrate the matching network into the design of the antenna gap itself; the outcome of this integration is shown in Figure 1.2. The name for this device also reflects the synthesis which was an integral part of the design process. According to Terman [6], the definition of balun is a "balancing unit". If this definition is combined with the addition of the antenna, *balancing unit plus antenna*, or *balantenna*, results. In effect the antenna feed region becomes the balun.

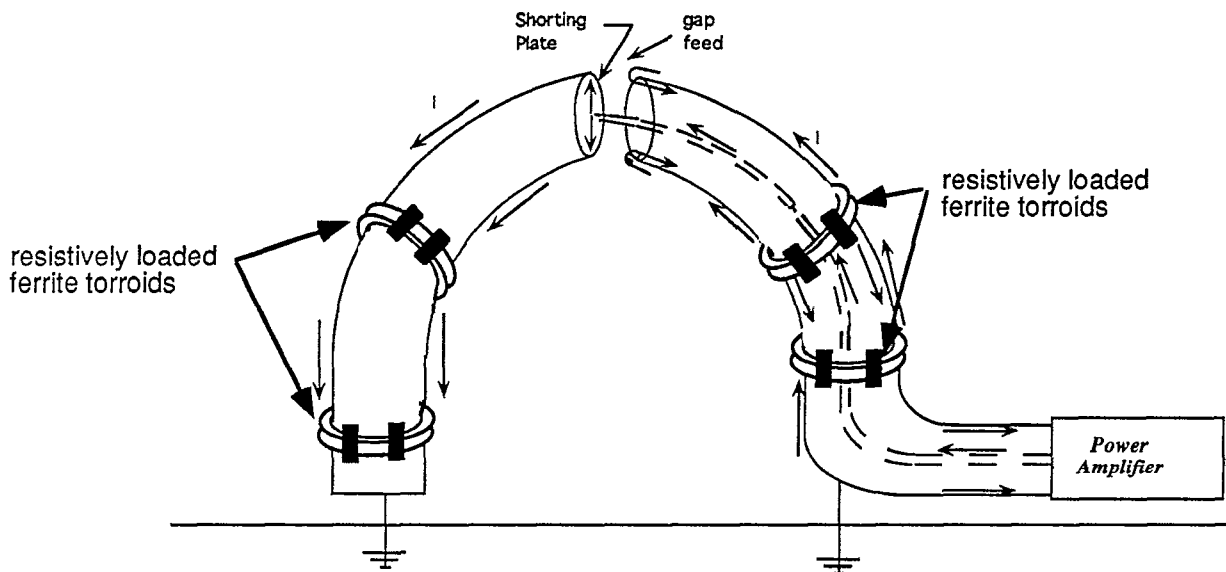


Figure 1.1. The "Wormhole" Feed for a Coaxial Cable Antenna

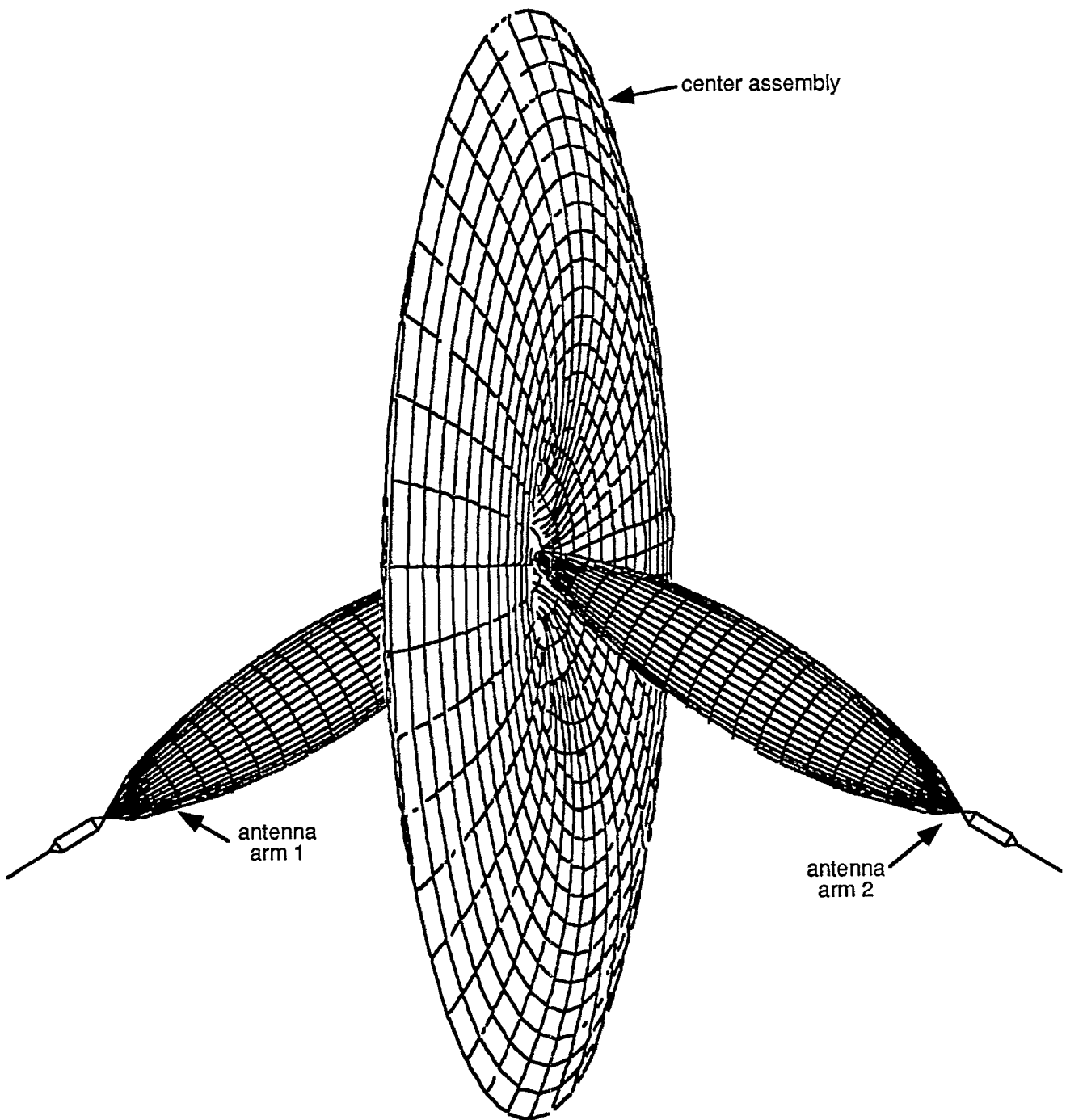


Figure 1.2. The Balantenna

## II. Description of the Balantenna

Figure 2.1 shows the internal design of the balantenna. The center assembly of the structure is a biconical body of revolution in the middle with the two circular cones deformed in a smooth way to rejoin at the outer edge of the plate. The plate is made of metal (aluminum), is approximately one meter in diameter and is hollow inside. A block of ferrite material is located inside this center plate. It is machined to follow the contours of the center assembly and the ferrite material is chosen for its high impedances over wide frequency ranges. Each arm of the antenna begins as a tilted monocone over the center assembly and gradually transitions into the coaxial cable which forms the remainder of the antenna arm. A dielectric structural-support-sphere holds the center plate and the two antenna arms in place with the proper alignment.

A small hole in the center assembly allows connections from the inner portion antenna coaxial cable feed to the individual arms and center assembly. (See the exploded detail in Figure 2.1.) The center conductor of the antenna feed coaxial cable is connected both to the opposite arm of the antenna and the surface "A" of the center plate. The shield of the feed coaxial cable is connected to the surface "B" of the center plate. As a general rule, all line lengths should be as small as possible; further, an attempt is made to "flair" the ends of the connections to the center assembly in such a way that impedances from the coaxial drive to the antenna elements are preserved.

In order to understand the fundamental operation of the Balantenna, it is instructive to compare it to a broadband coaxial cable balun (see Figure 2.2). In the case of the coaxial cable balun, a  $50\ \Omega$  feed is connected to two  $100\ \Omega$  coaxial cables in parallel. On one of the coaxial cables, a small Moebius gap [4] is formed, separating this cable into two segments. At the gap, the center conductor of one segment is connected to the shield of the other segment. This effectively reverses the polarity of the voltage wave traveling down the separated coaxial cable. The input feed is connected to the  $100\ \Omega$  coaxial cables in parallel and the antenna is connected to the  $100\ \Omega$  coaxial cables in series. (In other words, we have a single ended  $50\ \Omega$  input to differential  $200\ \Omega$  output.) This scheme matches the input feed impedance of  $50\ \Omega$  and an antenna impedance of  $200\ \Omega$ . The voltages on the input of the coaxial cables ( $V_0$ ) are conducted along the coaxial cables resulting in a voltage  $V_1$  at the output of the cables (to account for losses). The electrical length of these two paths are made to be the same, so as shown in the diagram, the voltages at the output of the coaxial cables are in phase, resulting in a  $2V_1$  voltage across the antenna. (Note that if this balun were in a shielded container, the ferrites on the non-gap coaxial cable would not be necessary.)

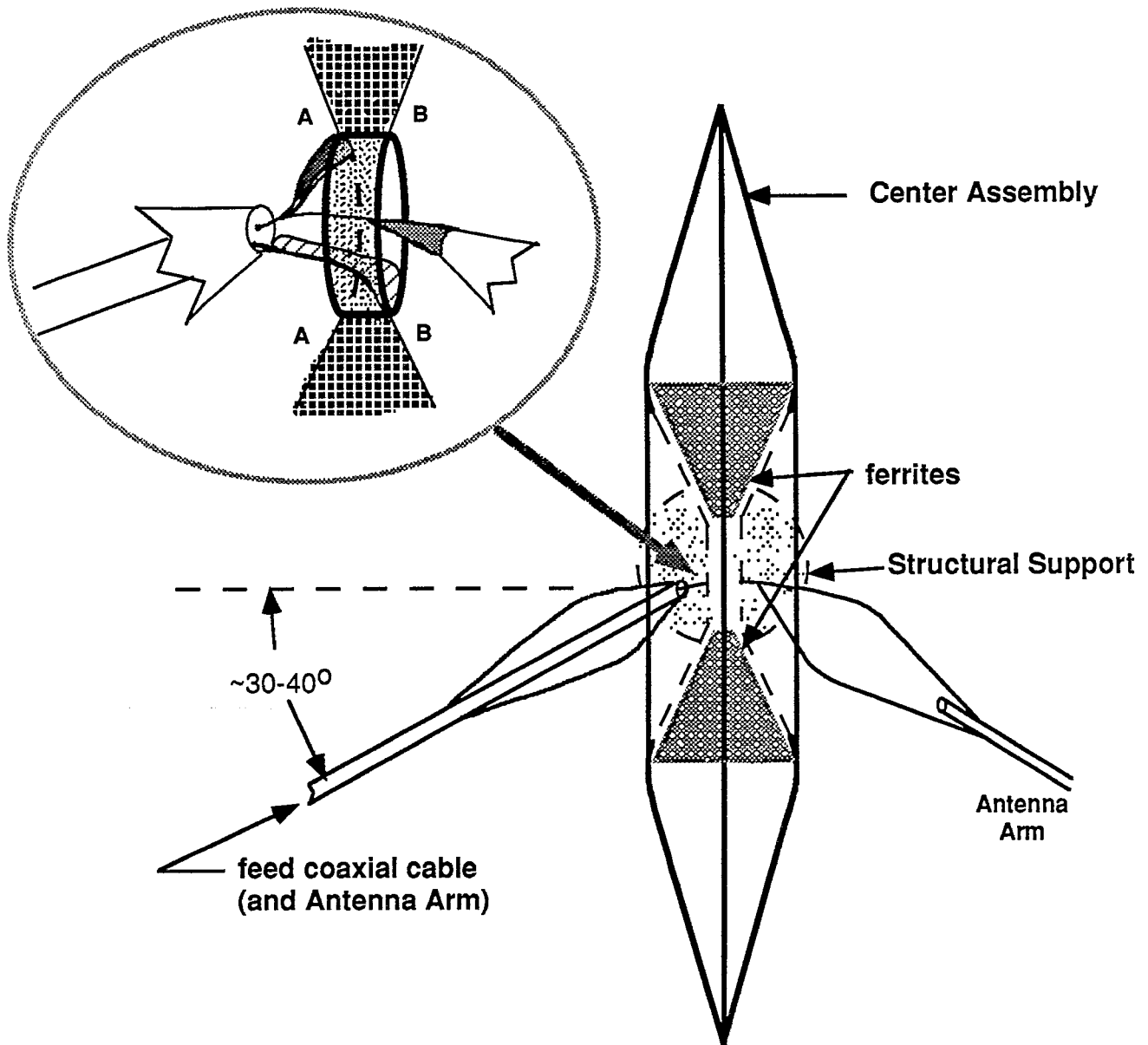
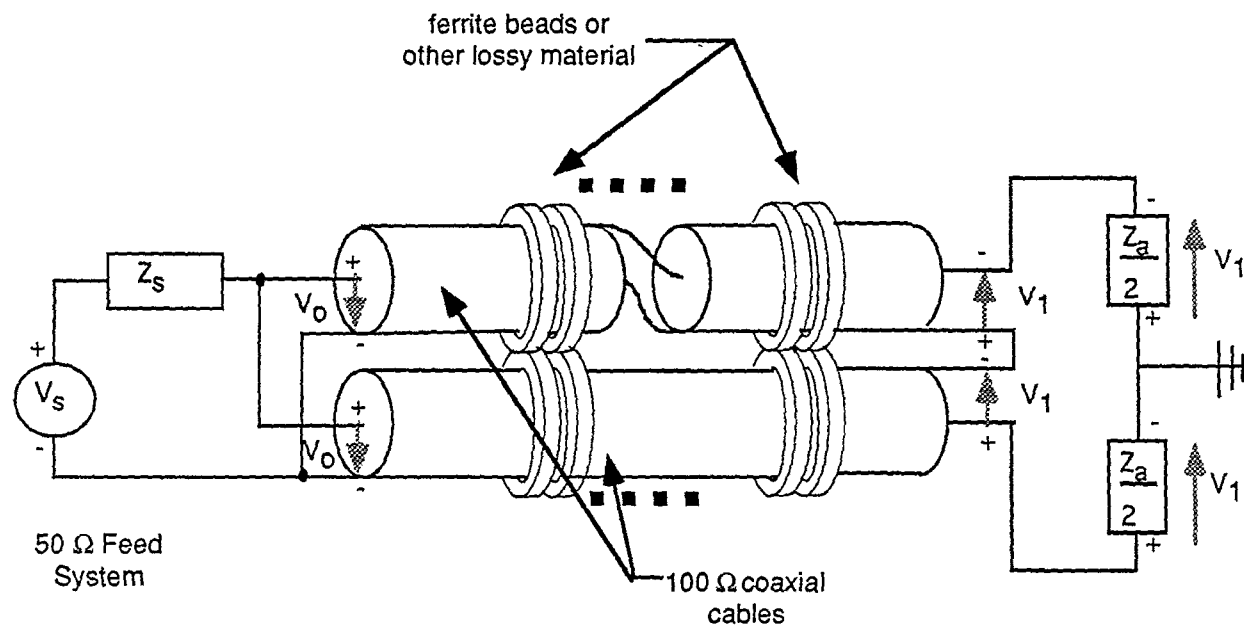
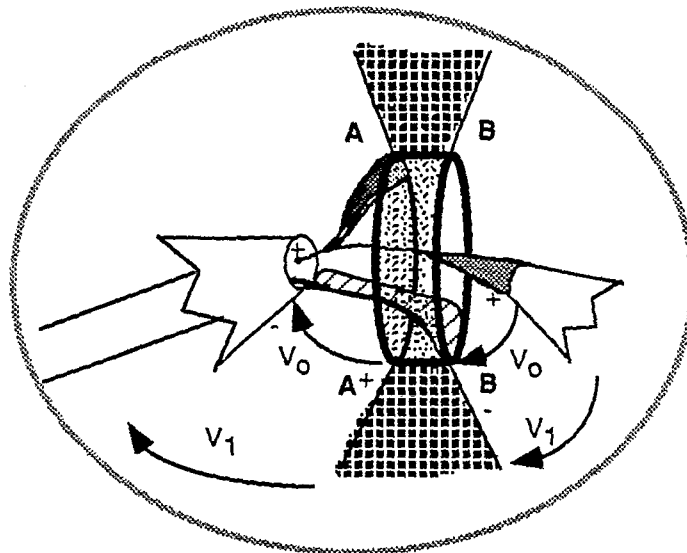


Figure 2.1. Internal details of the Balun antenna



(a) Voltages on a Coaxial Cable Balun



(b) The Voltages Generated on the Balantenna

Figure 2.2. Comparable Voltages on a Coaxial Cable Balun and the Balantenna

The three major features provided by the coaxial cable design are (1) isolation of absolute voltages through the coaxial cables, (2) the parallel input and series output of the signals input to and exiting the balun, respectively, and (3) the back impedance provided by the ferrite loading around the coaxial cables (preventing common mode currents on the outside of each coaxial cable shield which would result in short circuiting the output of the balun).

These design attributes are also reflected in the design of the Balantenna. The input voltage  $V_0$  is impressed across both monocone-bicone center plate input surfaces of the matching network (connected in parallel). The output voltage from the  $100 \Omega$  shaped surfaces,  $V_1$ , is impressed on each arm of the antenna in a series connection. These voltages,  $V_1$ , also lose their absolute reference by the action of the transmission lines. This serves the same function as in the coaxial cable design, with the impedance of the ferrites and the shaping of the center plate preventing a shorting current.

Finally, the arms of the antenna are directed downward approximately  $30-40^\circ$  to better concentrate the high frequency fields on objects below the antenna [7].

### III. Impedance of the Conical System

To determine the impedance of the conical system, consider the coordinate system shown in figure 3.1. In terms of the usually defined polar spherical coordinates, the half angle of the circular monocone (one antenna arm),  $\beta$ , and the angular displacement of the axis of this monocone from the z axis,  $\alpha$ , the equation of the monocone is

$$\cos \theta \cos \alpha + \sin \theta \sin \alpha \sin \phi = \cos \beta \quad (3.1)$$

For the biconical surface of revolution center assembly, we see from figure 3.1 that

$$\chi = 90 - \theta \quad (3.2)$$

Using techniques of stereographic projection previously described [8], the characteristics of the TEM mode wave propagating along the conical system can be determined by solving a Laplace equation over a spherical surface perpendicular to the propagation of the wave. This reduces to a two dimensional Laplace equation in the  $x', y'$  plane such that

$$x' = \cos(\phi) \tan\left(\frac{\theta}{2}\right), \quad y' = \sin(\phi) \tan\left(\frac{\theta}{2}\right) \quad (3.3)$$

The electric field along the conductors for the three-dimensional coordinate system is

$$\vec{E} = \frac{e^{\pm jkr}}{r} \nabla_t U(\theta, \phi) \quad (3.4)$$

with a corresponding magnetic field

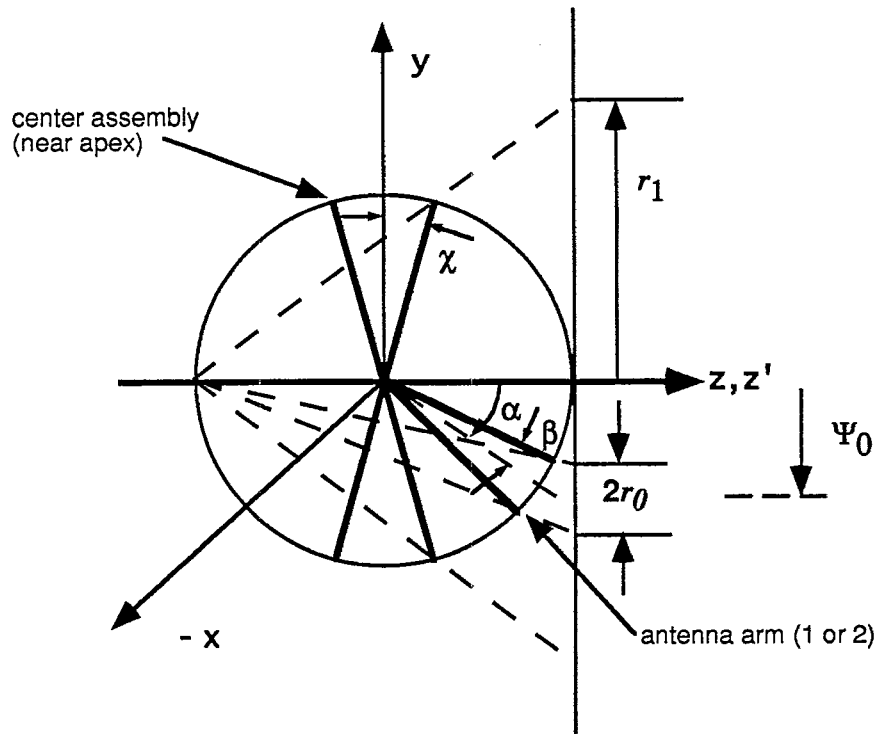
$$\vec{H} = \frac{e^{\pm jkr}}{Z_0 r} \bar{\mathbf{i}}_r \times \nabla_t U(\theta, \phi) = \frac{e^{\pm jkr}}{Z_0 r} \nabla_t V(\theta, \phi) \quad (3.5)$$

where the function  $U+jV$  is an analytic function of the variable  $e^{j\phi} \tan \frac{\theta}{2}$ . In these field equations the time dependence,  $e^{-j\omega t}$ , has been suppressed, and  $k = \frac{\omega}{c}$ . Further,  $\nabla_t$  is the transverse gradient, given by

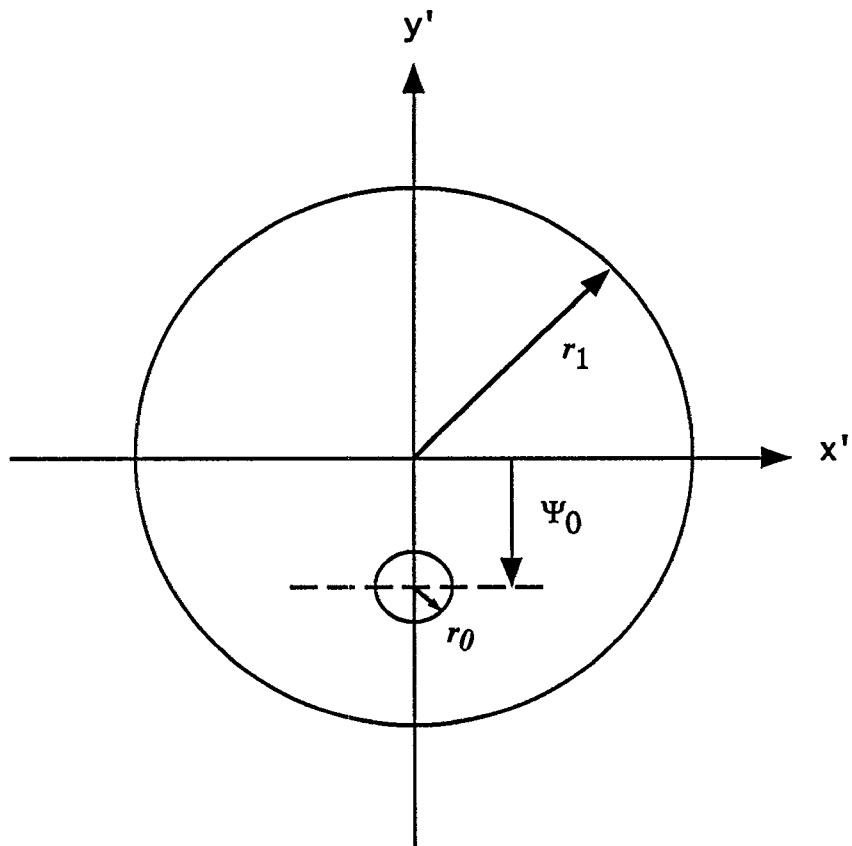
$$\nabla_t \equiv \bar{\mathbf{i}}_\theta \frac{\partial}{\partial \theta} + \frac{\bar{\mathbf{i}}_\phi}{\sin \theta} \frac{\partial}{\partial \phi}$$

$\bar{\mathbf{i}}_\theta \equiv$  unit vector in the  $\theta$  direction

$\bar{\mathbf{i}}_\phi \equiv$  unit vector in the  $\phi$  direction



(a) The Notation and Coordinate Systems for the Tilted Monocone Over the Center Assembly



(b) The Stereographic Projection

Figure 3.1. The Stereographic Projection of a Tilted Monocone Over the Center Assembly

Since the impedance of the monocone over the ground plane is the same as that of the impedance of the stereographic projections [8,9], the impedance of two cylindrical lines of different radii separated on centers by a known distance (see Figure 3.1 (b)) can be used to determine the impedance of these lines.

Now this monocone (antenna arm) over a biconical surface of revolution center assembly must have an impedance of  $100 \Omega$ ; thus, the task is to determine possible half angles for the monocone ( $\alpha$ ), angular displacements of the monocone ( $\beta$ ) and half angles of the center assembly ( $\chi$ ) which create this specific impedance.

Starting first with the stereographic projection of the monocone (antenna arm), let

$$\begin{aligned} \Psi^2 &= x'^2 + y'^2 \\ \text{so that } x' &= \Psi \cos(\phi), y' = \Psi \sin(\phi) \end{aligned} \quad (3.6)$$

we find from (3.1), (3.3) and (3.6) that

$$\frac{1 - \Psi^2}{1 + \Psi^2} \cos(\alpha) + \frac{2 \sin(\alpha)}{1 + \Psi^2} \Psi \frac{y'}{\Psi} = \cos(\beta) \quad (3.7)$$

and that

$$x'^2 + y'^2 - \frac{2y' \sin(\alpha)}{\cos(\alpha) + \cos(\beta)} + \frac{\sin^2(\alpha)}{[\cos(\alpha) + \cos(\beta)]^2} = \frac{\sin^2(\beta)}{[\cos(\alpha) + \cos(\beta)]^2} \quad (3.8)$$

or

$$x'^2 + (y' - \Psi_0)^2 = r_0^2 \quad (3.9)$$

where

$$\begin{aligned} \Psi_0 &= \frac{\sin(\alpha)}{\cos(\alpha) + \cos(\beta)} \\ \text{and} \end{aligned} \quad (3.10)$$

$$r_0 = \left[ \frac{\sin^2(\beta)}{[\cos(\alpha) + \cos(\beta)]^2} \right]^{1/2}$$

This turns out to be a circle in the  $x', y'$  plane whose radius is  $r_0$  and has a center which is offset from the origin by a distance  $\Psi_0$  along the  $y'$  axis (see figure 3.1).

For the center assembly circular cone, from (3.2)

$$\begin{aligned}\chi &= 90 - \theta \\ \text{thus } \sin(\chi) &= \cos(\theta)\end{aligned}$$

But we already know from (3.3) and (3.6) that

$$\cos(\theta) = \frac{1 - \Psi^2}{1 + \Psi^2} \quad (3.11)$$

so that

$$\sin(\chi) = \frac{1 - \Psi^2}{1 + \Psi^2} \quad (3.12)$$

and

$$x'^2 + y'^2 = r_1^2 \quad (3.13)$$

where

$$r_1 = \left[ \frac{1 - \sin(\chi)}{1 + \sin(\chi)} \right]^{\frac{1}{2}} \quad (3.14)$$

This also is a circle in the  $x', y'$  plane whose radius is  $r_1$  and whose center is at the origin of the  $x', y'$  plane (see figure 3.1).

The impedance of these infinitely-long cylinders whose projections in the  $x', y'$  plane are circles of different radii, one circle enclosing the other and whose separation of centers is  $\Psi_0$  can be found using standard transmission line techniques [8] as

$$\begin{aligned}Z &= \frac{Z_0}{2\pi} \operatorname{arccosh} \left[ \frac{r_1^2 + r_0^2 - \Psi_0^2}{2r_1 r_0} \right] \\ Z_0 &= \sqrt{\frac{\mu_0}{\epsilon_0}}\end{aligned} \quad (3.15)$$

where  $\mu_0$  and  $\epsilon_0$  are the magnetic permeability and dielectric constant of free space, respectively.

This can be simplified, using equations (3.10) and (3.14) as

$$Z = \frac{Z_0}{2\pi} \operatorname{arccosh} \left[ \frac{(1 + \zeta^2) \cos(\alpha) - (1 - \zeta^2) \cos(\beta)}{2\zeta \sin(\beta)} \right] \quad (3.16)$$

where

$$\zeta \equiv \sqrt{\frac{1 - \sin(\chi)}{1 + \sin(\chi)}}$$

Expressing this impedance as

$$Z = f_g Z_0$$

then

$$f_g = \frac{1}{2\pi} \operatorname{arccosh} \left[ \frac{(1 + \zeta^2) \cos(\alpha) - (1 - \zeta^2) \cos(\beta)}{2\zeta \sin(\beta)} \right] \quad (3.17)$$

We can now calculate a variety of combinations of the angles  $\alpha, \beta$  and  $\chi$  which result in a  $100 \Omega$  transmission line. Figure 3.2 shows such a combination of angles which will result in a  $100 \Omega$  system. Note that for an  $\alpha$  in the desired range of  $30^\circ$  to  $40^\circ$ , angles for  $\beta$  vary between  $18^\circ$  and  $23^\circ$  for angles of  $\chi$  between  $14^\circ$  and  $22^\circ$ .

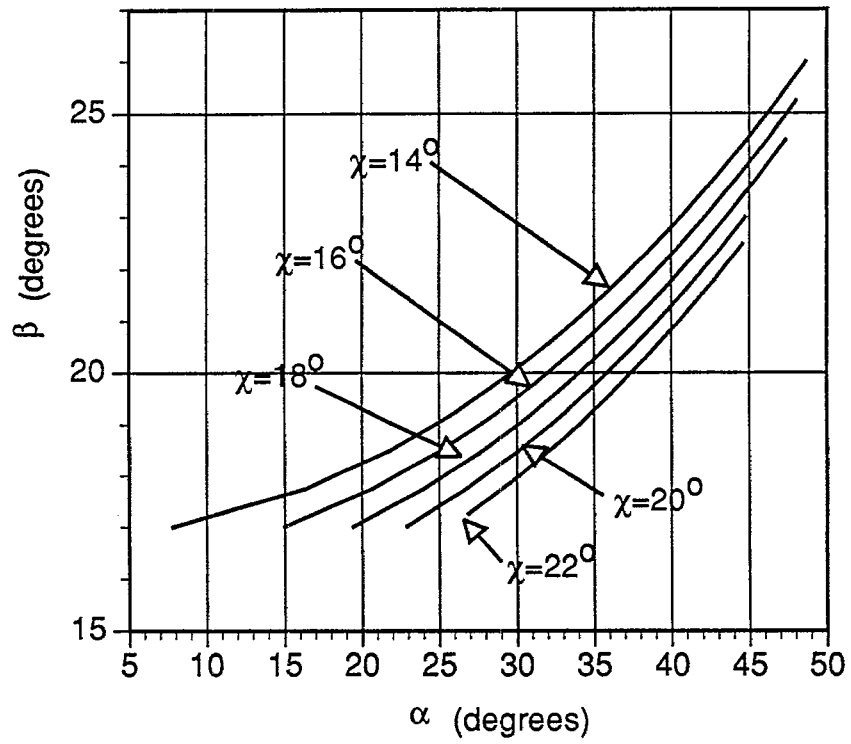


Figure 3.2. Various Combinations of angles for a 100  $\Omega$  System

#### IV. Conclusions

An integrated balun and antenna which will work for the "wormhole" feed antenna has been detailed in this note. This, combined with [1] describes the fundamental principals used to design a low weight, transportable CW hybrid simulator.

The loading achieved by the internal ferrites, as compared to the impedance of the antenna, and the connections between the drive coaxial cable and the ground plate and antenna arms will determine the overall performance of the balantenna. Combinations of ferrites can be used inside the ground plate to improve the low frequency and high frequency loading for currents on the ground plate. Careful shaping, sizing and positioning of the internal connections of the balantenna will influence the high frequency performance. With this care, the balantenna will match a 200  $\Omega$  load (differential), doubling the voltage on the output over a very broad frequency range. If the high frequency impedance of the antenna is significantly different from this value and amplifiers are used which are sensitive to impedance mismatches (low VSWR tolerances), additional shunt loading of the antenna can be used to make the balantenna work for this circumstance.

## V. References

1. C.E. Baum, W.D. Prather and D.P. McLemore, Topology for Transmitting Low-Level Signals from Ground Level to Antenna Excitation Position in Hybrid EMP Simulators, Sensor and Simulation Note 333, September 1991.
2. C.E. Baum, Winding Topology for Transformers, Measurement Note 31, October 2, 1986.
3. G.D. Sower and L.M. Atchley, Twin Coaxial Balun (TCB) Development, Measurement Note 34, June 3, 1987.
4. C.E. Baum, Winding Bundles for Transformers, Measurement Note 35, November 10, 1987.
5. E.C. Jordan and K.G. Balmain, Electromagnetic Waves and Radiating Systems, Prentice-Hall, New Jersey, 1968, pp 406-407.
6. Frederick E. Terman, Electrical and Radio Engineering. 4th Edition, McGraw Hill, 1955, pg 902.
7. Nickolas H. Younan and B. L. Cox, Gigahertz Analysis of the Elliptical Antenna, Sensor and Simulation Note 325, April 1990.
8. R. W. Latham, M.I. Sancer and A.D. Varvatsis, Matching A Particular Pulse to a Parallel-Plate Simulator, Circuit and Electromagnetic System Design Note 18, November 1974.
9. William R. Smythe, Static and Dynamic Electricity, Third Edition, Hemisphere Publishing Corporation, 1989